

Longitudinal Evaluation of Both Morphologic and Functional Changes in the Same Individuals with Alzheimer's Disease

Hiroshi Matsuda, MD¹; Noriyuki Kitayama, MD^{2,3}; Takashi Ohnishi, MD¹; Takashi Asada, MD⁴; Seigo Nakano, MD⁵; Shigeki Sakamoto, MD¹; Etsuko Imabayashi, MD¹; and Asako Katoh, MD¹

¹Department of Radiology, National Center Hospital for Mental, Nervous, and Muscular Disorders, National Center of Neurology and Psychiatry, Tokyo, Japan; ²Department of Radiology, University of Washington Medical Center, Seattle, Washington; ³Department of Psychiatry, Showa University School of Medicine, Tokyo, Japan; ⁴Department of Neuropsychiatry, Tsukuba University, Ibaraki, Japan; and ⁵Department of Geriatric Medicine, National Center Hospital for Mental, Nervous, and Muscular Disorders, National Center of Neurology and Psychiatry, Tokyo, Japan

Morphologic and functional imaging studies have not always given concordant results about brain areas showing atrophic changes and reduced flow or metabolism in Alzheimer's disease (AD). The aim of this study was to determine the initial abnormality and the longitudinal changes in both morphologic and functional measurements for the same individuals with AD.

Methods: We investigated 15 patients with mild AD and 25 age-matched healthy volunteers. The AD patients underwent both MRI and SPECT 3 times at intervals of approximately 1 y. The gray matter volume, as segmented from MRI, and the regional cerebral blood flow (rCBF), as measured by SPECT, of AD patients were compared with those of healthy volunteers using statistical parametric mapping, which is a voxel-based analysis in stereotactic space. **Results:** Considerable discordance between areas of regional atrophy and areas of decreased rCBF was observed. The medial temporal areas showed a faster and more extensive reduction of gray matter volume than of rCBF. In comparison with the value at the baseline study, rCBF in the posterior cingulate gyrus and precuneus and the associative parietal cortex was extensively decreased. In contrast, the extent of significant decrease in this area continued to be much narrower for gray matter volume than for rCBF, even in the follow-up studies. Frontal areas, including the anterior cingulate gyrus and the orbitofrontal areas, showed a progressive reduction in both rCBF and gray matter volume. The reduction in rCBF was in a more posterior part of the associative temporal cortex than was the reduction in gray matter volume. **Conclusion:** These results indicate a distinct discordance between morphologic and functional changes in a longitudinal study of AD. Functional changes may be caused partly by remote effects from the morphologically involved areas with decreased connectivity and partly by a compensatory response by neuronal plasticity.

Key words: Alzheimer's disease; SPECT; MRI; statistical parametric mapping

J Nucl Med 2002; 43:304–311

For diagnosing and evaluating the progression of Alzheimer's disease (AD), MRI and PET or SPECT are useful imaging modalities. However, the morphologic and the functional findings have not always been concordant. For instance, although patients with mild AD have been reported to show significant atrophy in the medial temporal structures (1,2), recent investigations have revealed significantly decreased glucose metabolism (3,4) or perfusion (5,6) not in the medial temporal structures but in the posterior cingulate gyrus and precuneus. This discordance cannot be clarified, because these findings were obtained from studies that used either MRI alone or PET or SPECT alone.

The aim of this study was to determine the initial abnormality and the longitudinal changes in both morphologic and functional measurements in the whole brain of the same individuals with AD. To study both changes not only in medial temporal structures but also in other brain areas, and to avoid subjectivity and adopt the principle of data-driven analysis, we applied a statistical parametric mapping (7) software program, which is a voxel-based analysis in stereotactic space.

MATERIALS AND METHODS

Subjects

Fifteen patients (11 men, 4 women; age range, 59–81 y; mean age \pm SD, 71.1 \pm 7.1 y) were identified from among consecutive new referrals to the memory clinic of the National Center Hospital for Mental, Nervous, and Muscular Disorders, National Center of Neurology and Psychiatry, between 1996 and 1999. The clinical diagnosis of AD was based on the *Diagnostic and Statistical Manual of Mental Disorders, 4th ed. (DSM-IV)* (8), and on the criteria of the National Institute of Neurological and Communica-

Received Sep. 11, 2001; revision accepted Dec. 3, 2001.

For correspondence or reprints contact: Hiroshi Matsuda, MD, Department of Radiology, National Center Hospital for Mental, Nervous, and Muscular Disorders, National Center of Neurology and Psychiatry, 4-1-1 Ogawahigashi, Kodaira, Tokyo, 187-8551, Japan.

E-mail: matsudah@ncnnp.musashi.jp

tive Disorders and Stroke and the Alzheimer's Disease and Related Disorders Association (9). Each patient underwent baseline SPECT and MRI at the time of the initial evaluation, was followed up clinically, and underwent second and third SPECT and MRI examinations at intervals ranging from 9 to 13 mo (11.4 ± 1.4 mo) and from 9 to 12 mo (11.9 ± 0.7 mo), respectively. At the time of baseline SPECT, the score of the Mini-Mental State Examination (MMSE) (10) was 21.5 ± 2.9 . At the time of follow-up SPECT 1 and 2 y later, the mean score declined to 19.1 ± 4.2 and 15.8 ± 5.7 , respectively. At the time of study entry, 3 of the 15 patients did not meet the DSM-IV criteria for AD (they had an MMSE score > 24). However, during the observation period, these 3 patients showed progressive cognitive decline and eventually fulfilled the criteria for AD.

Twenty-five healthy volunteers (16 men, 9 women; age range, 59–84 y; mean age, 71.2 ± 7.3 y) with no memory impairment or cognitive disorders served as control subjects. Each underwent SPECT and MRI once. Their performance was within normal limits both on the revised Wechsler Memory Scale (11) and on the revised Wechsler Adult Intelligence Scale (12). The MMSE score was 29.5 ± 0.6 . The healthy volunteers did not differ significantly from the AD patients in age or education. They had no close relatives with psychiatric or neurologic disorders. The ethics committee of the National Center of Neurology and Psychiatry approved this study for healthy volunteers, all of whom gave informed consent to participate.

All of the patients and healthy volunteers were screened by questionnaire and medical history to exclude those with medical problems potentially affecting the central nervous system, including a current or past neurologic disorder, head trauma with loss of consciousness, brain tumor, hypertension, heart disease, diabetes mellitus, Cushing's disease, steroid use, alcohol or drug abuse, epilepsy, schizophrenia, major depression, and posttraumatic stress disorder. In addition, in none was asymptomatic cerebral infarction detected by T2-weighted MRI.

Brain MRI Procedure

All MRI studies were performed on a 1.0-T system (Magnetom Impact Expert; Siemens, Erlangen, Germany). A 3-dimensional volumetric acquisition of a T1-weighted gradient echo sequence produced a gapless series of thin sagittal sections using an MPRage sequence (echo time/repetition time, 4.4/11.4; flip angle, 15° ; acquisition matrix, 256×256 ; 1 excitation; field of view, 31.5 cm; slice thickness, 1.23 mm).

Brain SPECT Procedure

Before SPECT was performed, an intravenous line was established in all subjects. While lying supine with eyes closed in a dimly lit, quiet room, each received an intravenous injection of 600 MBq ^{99m}Tc -ethyl cysteinate dimer. Ten minutes after this injection, brain SPECT was performed using a triple-head gamma camera (MULTISPECT3; Siemens, Hoffman Estates, IL) equipped with high-resolution fanbeam collimators. For each camera, projection data were obtained in a 128×128 format for 24 angles of 120° at 50 s per angle. A Shepp and Logan Hanning filter was used for SPECT image reconstruction at 0.7 cycle per centimeter. Attenuation correction was performed using Chang's method.

Image Analysis

Voxel-based morphometry for an MR image was performed as described in our previous study (13). The theory and algorithm of

this voxel-based morphometry were well documented by Ashburner and Friston (14). The acquired MR images were reformatting to gapless 2-mm-thick transaxial images. Images were analyzed using Statistical Parametric Mapping 99 (SPM99) (Wellcome Department of Cognitive Neurology, London, U.K.) running on MATLAB (The MathWorks, Inc., Sherborn, MA). Spatial normalization fitted each individual brain to a standard template brain (Talairach and Tournoux (15)) in 3-dimensional space, so as to correct for differences in brain size and shape and facilitate intersubject averaging. In spatial normalization, only 12-parameter affine transformation was used to avoid segmentation errors caused by partial-volume effects inherently created by warping (16). Normalized MR images were then segmented into gray matter, white matter, cerebrospinal fluid, and other compartments using a modified version of the clustering algorithm, the maximum likelihood "mixture model" algorithm (14,17). The segmentation procedure involves calculating for each voxel a Bayesian probability of belonging to each tissue class based on a priori MRI information with a nonuniformity correction (14,17). The segmented gray matter images were then subjected to an affine and nonlinear spatial normalization. The spatially normalized gray matter images were smoothed with an isotropic gaussian kernel 12 mm in full width at half maximum (FWHM) to use the partial-volume effect to create a spectrum of gray matter intensities. The gray matter intensities are equivalent to the weighted average of gray voxels located in the volume fixed by the smoothing kernel. Regional intensities can therefore be taken as equivalent to gray matter volumes (14).

Voxel-based analysis of SPECT data was performed also using SPM99. The images were spatially normalized using SPM99 to an original template for ^{99m}Tc -ethyl cysteinate dimer (18). Then, images were smoothed with a gaussian kernel 12 mm in FWHM.

Statistical Analysis

The processed images were analyzed using SPM99, which implements a general linear model. The overall mean of gray matter volume and global cerebral blood flow was treated as a confounding covariate. A proportional scaling routine was used to achieve global normalization of voxel values between scans.

We studied differences in gray matter volume and regional cerebral blood flow (rCBF) between AD patients and age-matched healthy volunteers using *t* statistics. The resulting sets of *t* values constituted statistical parametric maps (SPM(*t*)). The SPM(*t*) were transformed to the unit normal distribution (SPM(*Z*)) and were subjected to a threshold of $P < 0.001$. To correct for multiple nonindependent comparisons inherent in this analysis, the resulting foci were then characterized in terms of their spatial extent. This characterization is in terms of the probability that a region of the observed number of voxels, or more, could have occurred by chance over the entire volume analyzed. The significance of each region was estimated with a threshold of $P = 0.05$ using distributional approximations from the theory of gaussian fields (7). Anatomic localization was according to the atlas of Talairach and Tournoux (15) using a set of linear transformations (19).

RESULTS

Figure 1 and Table 1 show the location and peaks of significant reduction of gray matter volume in AD patients compared with healthy volunteers. The gray matter volume was significantly reduced in both temporal gyri, both frontal

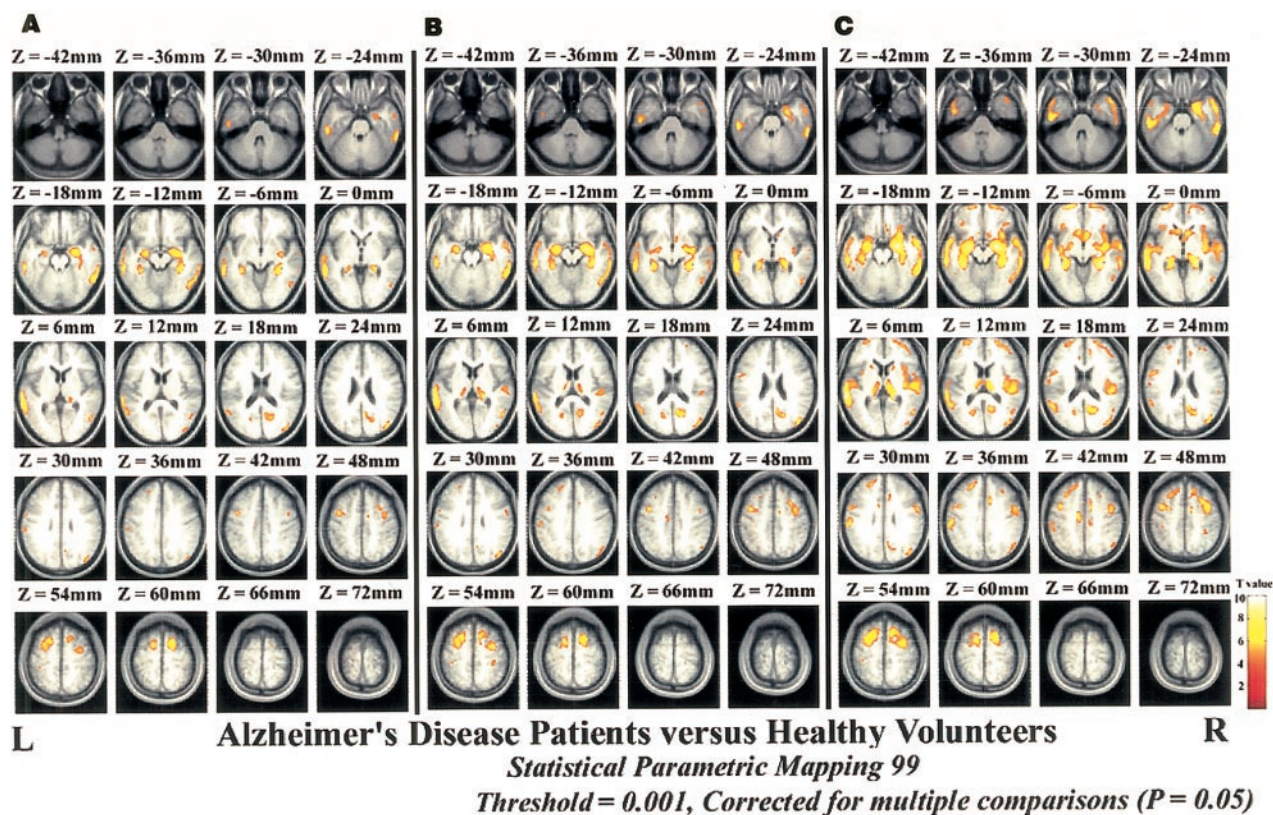


FIGURE 1. SPM99 corrected for multiple comparisons ($P = 0.05$). Images show significantly lower ($P = 0.001$) gray matter volume in AD patients, in comparison with that in healthy volunteers, at baseline (A) and at 1-y (B) and 2-y (C) follow-up. Significant decrease is shown as colored areas superimposed on transaxial slices of standard MR images.

gyri, both amygdala, the right parahippocampal gyrus, the left fusiform gyrus, the right posterior cingulate gyrus, and the left precuneus at the baseline study. Significantly reduced areas subsequently spread to surrounding areas with further involvement of both thalami, both anterior cingulate gyri, both heads of caudate nucleus, and the right parietal lobe from the 1-y to 2-y follow-up studies.

Figure 2 and Table 2 show the location and peaks of significant reduction of rCBF in AD patients compared with healthy volunteers. The rCBF was significantly reduced in both precuneus, both parietal lobules, both frontal gyri, the right hippocampus, the left parahippocampal gyrus, the right rectal gyrus, the right posterior cingulate gyrus, and the left angular gyrus at the baseline study. Significantly reduced areas gradually spread to surrounding areas from the 1-y to 2-y follow-up studies, with further involvement of both thalami, both anterior cingulate gyri, the right fusiform gyrus, and both occipital gyri.

A comparison of the extent of significantly decreased gray matter volume with that of decreased rCBF is shown in Figure 3. In the medial temporal areas, the gray matter volume was widely decreased at the baseline study, with this decrease extending to the surrounding areas in the follow-up studies. In contrast, the rCBF decreased in much narrower and more posterior regions of the medial temporal areas than did gray matter volumes, and this decrease grad-

ually extended from the posterior to the anterior portion as the disease progressed. The posterior cingulate gyrus and precuneus and the parietal lobules showed extensively decreased rCBF at the baseline study. These areas showed an exceedingly limited extent of decreased gray matter volume even in the 2-y follow-up study. The associative temporal cortex showed a reduction of rCBF in a more posterior part than that of the reduced gray matter volume at baseline, and the reduction gradually extended to the anterior part in follow-up studies.

DISCUSSION

Most previous pathologic studies suggested that structures within the medial temporal areas, amygdala, hippocampal formation, entorhinal cortex, and parahippocampal and fusiform gyri are initially affected in AD with histologic changes, including amyloid deposits and neurofibrillary changes (20–22). The reduced rCBF in the medial temporal structures of patients with mild to moderate AD shown by a recent high-resolution SPECT system (23–25) is consistent with these pathologic findings. Our longitudinal SPECT study (6) also revealed significant flow reductions in the medial temporal area when the mean MMSE score was 22.3. Moreover, our MRI study (13) revealed a significant reduction of gray matter volume in the hippocampal forma-

TABLE 1
Location and Peaks of Significant Decreases in Gray Matter Volume

Study	Structure	Coordinates			z score
		x	y	z	
Baseline of AD patients versus healthy volunteers	Left superior temporal gyrus	−63	−33	9	6.75
	Right inferior temporal gyrus	59	−49	−13	6.69
	Right amygdala	26	−6	−11	6.52
	Right parahippocampal gyrus	36	−35	−5	6.48
	Right hippocampus	32	−39	−1	6.39
	Right superior frontal gyrus	18	7	57	6.34
	Left amygdala	−24	−8	11	5.87
	Right middle temporal gyrus	46	−73	26	5.79
	Left middle frontal gyrus	−40	4	44	5.79
	Left fusiform gyrus	−34	−37	−7	5.59
	Left hippocampus	−32	−36	−6	5.59
	Right posterior cingulate gyrus	8	−53	23	5.25
	Left precuneus	−20	−63	16	5.11
1-y follow-up of AD patients versus healthy volunteers	Right amygdala	26	−6	−11	7.27
	Left superior temporal gyrus	−63	−33	9	7.22
	Right hippocampus	30	−39	−1	6.80
	Left amygdala	−24	−8	−10	6.52
	Right inferior temporal gyrus	59	−49	−13	6.49
	Right superior frontal gyrus	18	7	55	6.14
	Right middle temporal gyrus	46	−73	26	6.05
	Left middle frontal gyrus	−40	6	40	5.94
	Left hippocampus	−32	−37	−3	5.93
	Right precuneus	16	−61	20	5.64
	Right posterior cingulate gyrus	8	−53	21	5.51
	Left precuneus	−20	−63	16	5.58
	Left postcentral gyrus	−55	−20	34	5.00
	Left anterior cingulate gyrus	−10	−12	39	4.86
	Right thalamus	12	−14	12	4.84
	Left thalamus	−14	−15	10	4.83
	Right inferior parietal lobule	51	−60	38	4.79
	Left inferior frontal gyrus	−50	5	20	4.72
	Right middle frontal gyrus	24	55	12	4.55
	Right anterior cingulate gyrus	10	15	32	4.49
2-y follow-up of AD patients versus healthy volunteers	Right amygdala	26	−6	−13	7.82
	Left inferior temporal gyrus	−63	−33	9	7.74
	Right hippocampus	30	−39	−1	7.64
	Left amygdala	−24	−8	−11	7.40
	Left hippocampus	−32	−35	−7	6.90
	Left middle frontal gyrus	−26	2	48	6.36
	Left anterior cingulate gyrus	−10	−12	39	6.06
	Right thalamus	12	−19	8	5.98
	Right caudate nucleus (head)	8	13	−4	5.94
	Right posterior cingulate gyrus	8	−53	21	5.93
	Left posterior cingulate gyrus	−20	−61	16	5.75
	Right middle temporal gyrus	44	−74	26	5.72
	Right precuneus	18	−61	21	5.69
	Left caudate nucleus (head)	−6	13	−6	5.68
	Right superior frontal gyrus	20	62	−1	5.38
	Left thalamus	−14	−17	10	5.37
	Right medial frontal gyrus	12	40	16	5.31
	Right insula	38	10	−2	5.18
	Left inferior frontal gyrus	−36	31	−10	5.06
	Left postcentral gyrus	−38	−29	49	4.94
	Right medial frontal gyrus	8	28	−18	4.79
	Right inferior parietal lobule	34	−38	48	4.70
	Left insula	−40	−24	18	4.45

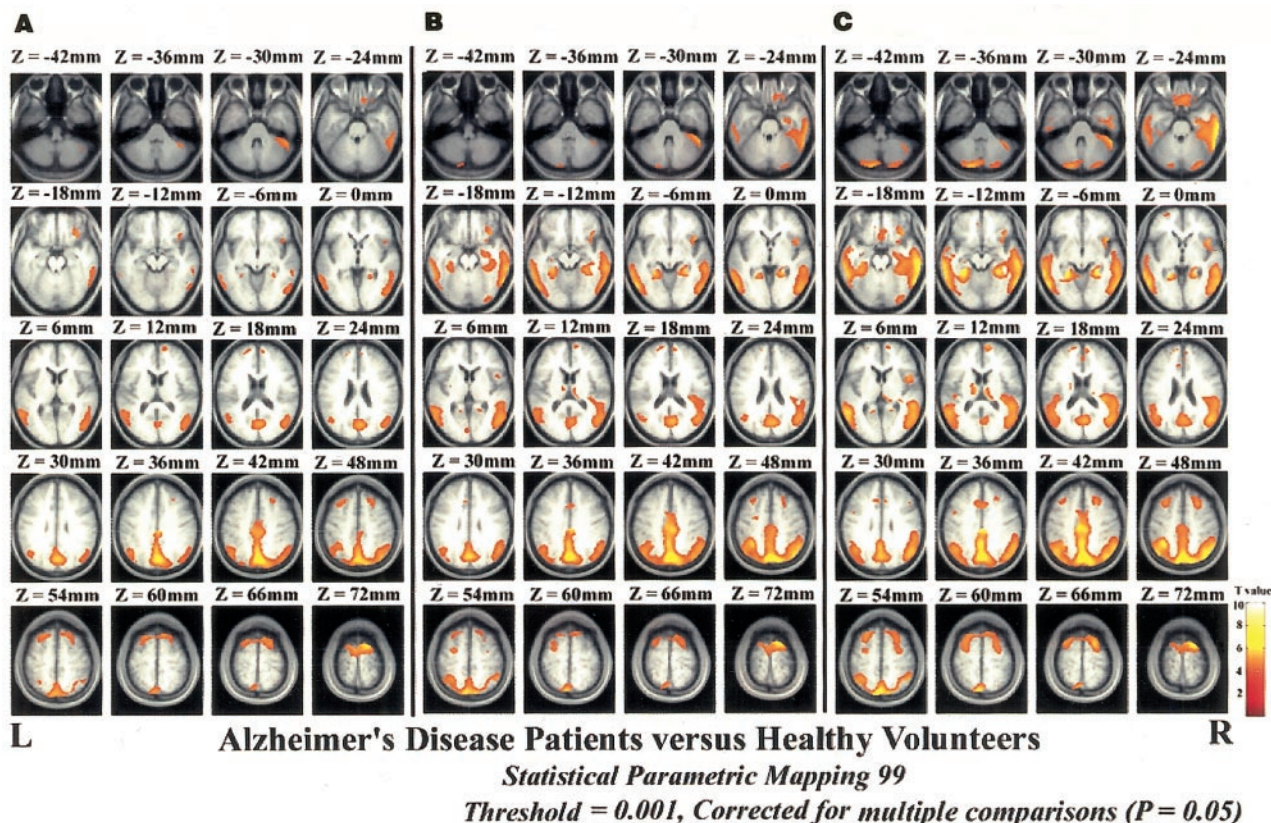


FIGURE 2. SPM99 corrected for multiple comparisons ($P = 0.05$). Images show significantly lower ($P = 0.001$) adjusted rCBF in relative flow distribution (normalization of global cerebral blood flow for each subject to 50 mL/100 g/min with proportional scaling) in AD patients, in comparison with that in healthy volunteers, at baseline (A) and at 1-y (B) and 2-y (C) follow-up. Significant decrease is shown as colored areas superimposed on transaxial slices of standard MR images.

tion and entorhinal cortex bilaterally in AD patients with a mean MMSE score of 20.7. Recent voxel-based morphometry of MRI in patients with mild AD also revealed a significant decrease in the hippocampus (13,16,26). The reduction of rCBF in the hippocampus may be caused not solely by a partial-volume effect but also by the disease process in AD. The reduction of rCBF is mild in comparison with that of volume. Julin et al. (24) reported a much greater reduction in gray matter volume (39.6%) than in hippocampal blood flow (12.0%) in patients with mild to moderate AD compared with healthy volunteers. Our cross-sectional study (27) on both anatomic and functional measurements in the same individuals also revealed less decline in rCBF (16.7%) than in volume (21.8%) in the hippocampus of patients with early AD compared with healthy volunteers.

On the other hand, our longitudinal study (6) did not find a significant decrease in hippocampal blood flow in patients with very early AD with a mean MMSE score of 26.2. In patients with mild to moderate AD, Ishii et al. (28) found that PET showed no significant rCBF decrease in spite of atrophy in the hippocampus. Ibanez et al. (29) also reported no significant decreases in glucose metabolism in the medial temporal structures of AD patients. This study showed that the medial temporal structures with significantly decreased

rCBF were much narrower and more posterior than those with decreased gray matter volume. These findings suggest that medial temporal structures show functional reductions to a lesser degree than does atrophy in very mild to moderate AD. This discordance may result from a plastic response in AD. The perforant path, which arises from the entorhinal cortex and has been reported to be the first affected in AD (22), is the major cortical input to the hippocampus. The neuronal loss in the entorhinal cortex of AD patients appears to act as a stimulus in a similar manner to that of the lesion in the rat brain, where loss of a set of axons induces sprouting of the remaining afferents and replacement of the lost connections to maintain synaptic activity (30,31). This compensatory response of reinnervation in the course of AD would result in milder functional changes than morphologic changes.

In a very early stage of AD, even before a clinical diagnosis of probable AD is possible, decreases of rCBF and glucose metabolism in the posterior cingulate gyri and precuneus have been reported using PET (3,4) and SPECT (5,6). In mild to moderate AD, investigations (29,32) also reported reductions of rCBF or glucose metabolism in this area, as was shown by this study. Reduced PET measures of glucose metabolism in this area persist even after partial-

TABLE 2
Location and Peaks of Significant Decreases in Adjusted rCBF

Study	Structure	Coordinates			z score
		x	y	z	
Baseline of AD patients versus healthy volunteers	Right and left precunei	0	-56	40	5.84
	Right inferior parietal lobules	40	-67	44	5.25
	Left superior frontal gyrus	-8	0	68	5.16
	Right inferior frontal gyrus	34	26	-18	4.85
	Left inferior parietal lobules	-44	-58	40	4.83
	Right superior frontal gyrus	12	9	68	4.67
	Right medial frontal gyrus	12	61	10	4.57
	Right hippocampus	26	-41	0	4.54
	Right rectal gyrus	12	26	-23	4.39
	Left parahippocampal gyrus	-30	-41	-5	4.25
	Right posterior cingulate gyrus	4	-2	37	4.13
	Left angular gyrus	-40	-72	33	4.05
1-y follow-up of AD patients versus healthy volunteers	Right and left precunei	0	-70	42	6.14
	Right and left posterior cingulate gyri	0	-18	36	5.64
	Right inferior parietal lobules	40	-67	45	5.54
	Left parahippocampal gyrus	-28	-37	-5	5.48
	Right inferior frontal gyrus	46	15	-6	5.21
	Left superior frontal gyrus	-6	-6	70	5.16
	Right superior frontal gyrus	12	9	68	4.94
	Left inferior parietal lobules	-42	-62	44	4.93
	Left hippocampus	-32	-26	-12	4.68
	Right parahippocampal gyrus	30	-11	-15	4.63
	Right medial frontal gyrus	10	57	14	4.54
	Left thalamus	-8	-11	12	4.53
	Right inferior occipital gyrus	34	-86	-14	4.53
	Right thalamus	16	-27	12	4.45
	Right fusiform gyrus	22	-90	-16	4.23
	Right middle frontal gyrus	32	-3	50	4.07
	Right transverse temporal gyrus	34	-31	7	4.06
	Left anterior cingulate gyrus	-6	26	23	4.06
	Left middle occipital gyrus	-28	-89	3	4.04
2-y follow-up of AD patients versus healthy volunteers	Left parahippocampal gyrus	-30	-41	-5	6.30
	Bilateral precunei	0	-68	40	6.18
	Right inferior temporal gyrus	63	-26	-19	6.16
	Right inferior parietal lobules	40	-63	44	5.93
	Right hippocampus	26	-39	-1	5.90
	Right and left posterior cingulate gyri	0	-18	36	5.87
	Left inferior parietal lobules	-42	-62	45	5.51
	Right medial frontal gyrus	12	61	10	5.24
	Right superior frontal gyrus	20	9	66	5.10
	Left thalamus	-12	-13	14	5.13
	Right rectal gyrus	10	26	-23	4.84
	Left rectal gyrus	-2	18	-21	4.61
	Left medial frontal gyrus	-10	59	15	4.41
	Left superior frontal gyrus	-26	58	-3	4.26
	Left inferior frontal gyrus	-48	7	29	4.18
	Left middle temporal gyrus	-48	-5	-15	4.04
	Right fusiform gyrus	18	-92	-12	4.04
	Right anterior cingulate gyrus	2	25	5	4.03

volume effects are taken into account; thus, the reduction is more than just an artifact resulting from an increase in cerebral fluid space (29). The observation that metabolic reduction in this area predicts cognitive decline in presymptomatic persons indicates that the pathophysiologic process

begins well before even mild or questionable dementia is recognized clinically (33). PET measures of glucose hypometabolism reflect decreased synaptic activity caused either by loss or by dysfunction of synapses (34), and regional metabolic deficits observed on PET may reflect projections

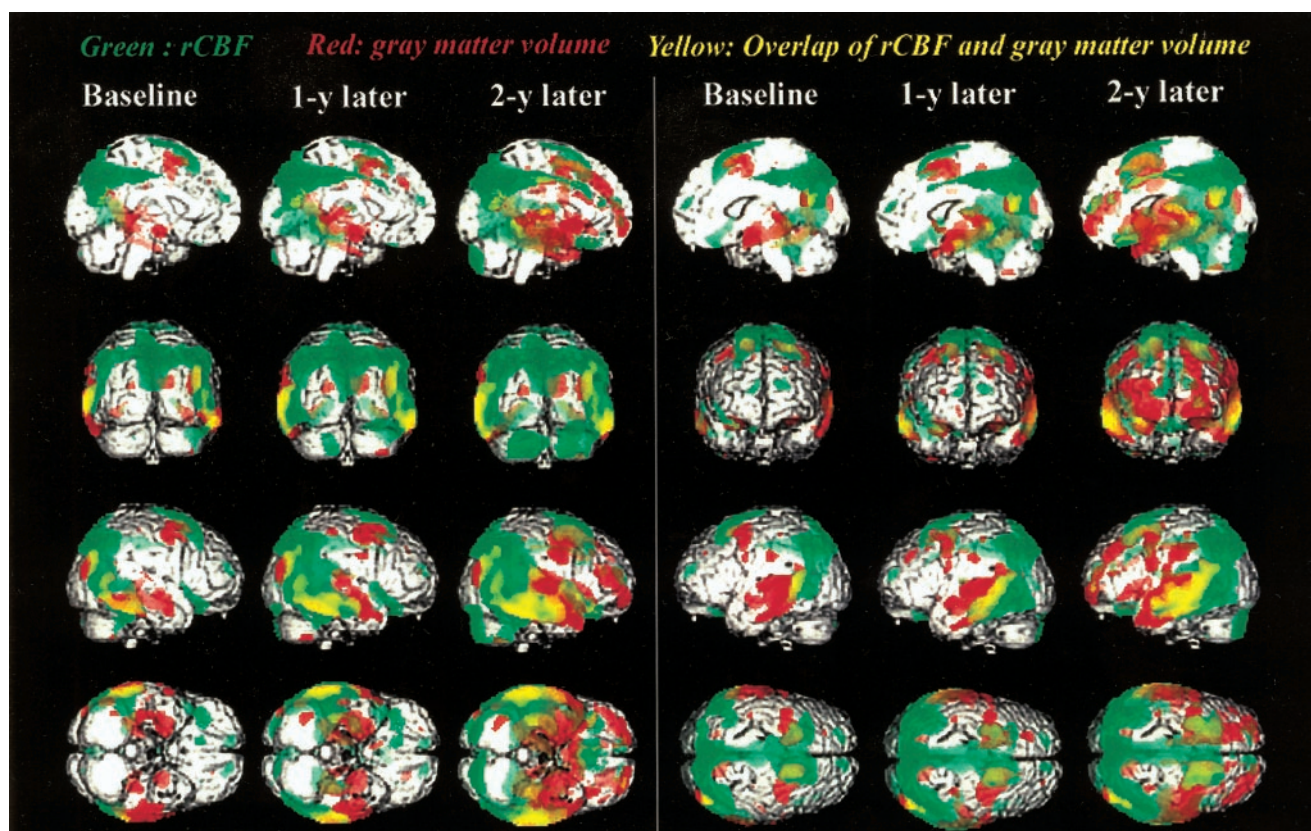


FIGURE 3. SPM99 corrected for multiple comparisons ($P = 0.05$). Dual-color display of surface-rendered standard MR images from 8 viewpoints shows significantly lower ($P = 0.001$) gray matter volume (red) and rCBF (green) in AD patients, in comparison with those in healthy volunteers. Areas of overlap are indicated by yellow.

from dysfunctional neurons in other brain lesions. In non-human primates, lesions of the entorhinal cortex cause a significant and long-lasting metabolic decline in a small set of remote brain regions, especially in the inferior parietal, posterior temporal, posterior cingulate, and associative occipital cortices and in the posterior hippocampal regions (35). These results suggest that flow or metabolic reduction in the posterior cingulate gyrus and precuneus indicates the earliest functional changes in AD as a remote effect caused by neuroanatomic disconnection with the rhinal cortex.

The region containing the posterior cingulate gyrus and precuneus is known to be important in memory (36). The retrosplenial cortex receives input from the subiculum and projects to the anterior thalamus, thus providing an alternative route between the hippocampus and thalamus. Medial temporal structures involved in memory receive anterior thalamic input directly through the cingulate bundle and indirectly through a relay in the retrosplenial cortex (37). This thalamocortical portion of the circuit of Papez (38) may be important in memory, and lesions of the cingulum and retrosplenial cortex may cause memory dysfunction by disrupting this pathway. A PET study also showed activation in the precuneus during episodic memory retrieval tasks (36).

Many researchers have shown metabolic and blood flow reductions in the parietotemporal association cortex (39).

This finding has been widely recognized as a diagnostic pattern for AD. The current rCBF reduction in the extensive associative parietal cortex without extensive atrophy agreed well with a previous PET study (40). In the associative temporoparietal cortex, glucose metabolism showed a significant decrease without regional tissue loss as assessed by ^{11}C -methionine accumulation. The associative frontal cortex is reduced in certain patients, often those with advanced AD (39). Several investigators have consistently addressed spread to the frontal lobes in longitudinal changes of functional alteration in the cerebral cortex of AD (39), as was shown in this study. In frontal areas, the anterior cingulate gyrus and orbitofrontal areas were also involved. Decreased rCBF in the anterior cingulate gyrus has been reported in patients with questionable AD at baseline SPECT who converted to AD on follow-up (5). After involvement of the medial temporal structures, neuropathologic changes of neurofibrillary tangles spread to the basal forebrain and anterior cingulate before encroaching on the neocortical association areas (20,41). The posterior location of reduced rCBF, in comparison with the location of reduced gray matter volume, in the associative temporal lobes may indicate that the reduced rCBF is caused by a remote effect (35). Our findings suggesting reduction of both rCBF and gray matter volume in the thalamus and caudate nuclei in an advanced stage are consistent with neuropathologic findings

(20) and previous reports using voxel-based morphometry of MRI in AD (16,26).

CONCLUSION

The SPM99 analysis showed discordance of morphologic and functional changes in a longitudinal study of patients with mild AD, prominently in the medial temporal areas, the posterior cingulate gyri and precunei, and the associative parietal cortex. The medial temporal areas showed a greater reduction in gray matter volume than in rCBF. In contrast, the posterior cingulate gyri and precunei and the associative parietal cortex showed a greater reduction in rCBF than in gray matter volume. These findings may indicate that remote effects, with decreased connectivity and a compensatory response to morphologic involvement, are responsible for functional changes in AD.

ACKNOWLEDGMENTS

The authors thank the technical staff in their hospital for data acquisition; Katsuyoshi Mizukami, MD, of the Department of Neuropsychiatry, Tsukuba University, for his valuable suggestion; and John Gelblum for his proofreading of the manuscript.

REFERENCES

- Jack CR, Petersen RC, Xu YC, et al. Medial temporal atrophy on MRI in normal aging and very mild Alzheimer's disease. *Neurology*. 1997;49:786–794.
- Bobinski M, Leon MJ, Convit A, et al. MRI of entorhinal cortex in mild Alzheimer's disease. *Lancet*. 1999;353:38–40.
- Minoshima S, Foster NL, Kuhl DE. Posterior cingulate cortex in Alzheimer's disease [letter]. *Lancet*. 1994;344:895.
- Minoshima S, Giordani B, Berent S, et al. Metabolic reduction in the posterior cingulate cortex in very early Alzheimer's disease. *Ann Neurol*. 1997;42:85–94.
- Johnson KA, Jones BL, Holman JA, et al. Preclinical prediction of Alzheimer's disease using SPECT. *Neurology*. 1998;50:1563–1571.
- Kogure D, Matsuda H, Ohnishi T, et al. Longitudinal evaluation of early Alzheimer's disease using brain perfusion SPECT. *J Nucl Med*. 2000;41:1155–1162.
- Frith CD, Friston KJ, Ashburner J, et al. Principles and methods. In: Frackowiak RSJ, Friston KJ, Frith CD, Dolan RJ, Mazziotta JC, eds. *Human Brain Function*. San Diego, CA: Academic Press; 1997:3–159.
- Diagnostic and Statistical Manual of Mental Disorders, 4th ed. (DSM-IV)*. Washington, DC: American Psychiatric Association; 1994:123–163.
- McKhann G, Drachman D, Folstein M, Katzman R, Price D, Stadlan EM. Clinical diagnosis of Alzheimer's disease: report of the NINCDS-ADRDA work group under the auspices of Department of Health and Human Services task force on Alzheimer's disease. *Neurology*. 1984;34:939–944.
- Folstein MF, Folstein SE, McHugh PR. Mini-Mental State: a practical method for grading the cognitive state of patients for the clinician. *J Psychiatr Res*. 1975;12:189–198.
- Wechsler D. *Wechsler Memory Scale: Revised Manual*. San Antonio, TX: Psychological Corp.; 1987.
- Wechsler D. *The Wechsler Adult Intelligence Scale, Revised*. New York, NY: Psychological Corp.; 1981.
- Ohnishi T, Matsuda H, Tabira T, Asada T, Uno M. Changes in brain morphology in Alzheimer's disease and normal aging: is Alzheimer's disease an exaggerated aging process? *AJNR*. 2001;22:1680–1685.
- Ashburner J, Friston KJ. Voxel-based morphometry: the methods. *Neuroimage*. 2000;11:805–821.
- Talairach J, Tournoux P. *Co-Planar Stereotaxic Atlas of the Human Brain*. Stuttgart, Germany: Thieme; 1988.
- Baron JC, Chetelat G, Desganges B, et al. In vivo mapping of gray matter loss with voxel-base morphometry in mild Alzheimer's disease. *Neuroimage*. 2001;14:298–309.
- Ashburner J, Friston K. Multimodal image coregistration and partitioning: a unified framework. *Neuroimage*. 1997;6:209–217.
- Ohnishi T, Matsuda H, Hashimoto T, et al. Abnormal regional cerebral blood flow in childhood autism. *Brain*. 2000;123:1838–1844.
- Brett M. The MNI Brain and the Talairach Atlas. Available at: www.mrc-cbu.cam.ac.uk/Imaging/mnispace.html. Accessed January 16, 2002.
- Braak H, Braak E. Neuropathological staging of Alzheimer-related changes. *Acta Neuropathol (Berl)*. 1991;82:239–256.
- Braak H, Braak E. Staging of Alzheimer's disease-related neurofibrillary changes. *Neurobiol Aging*. 1995;16:271–284.
- Gomez-Isla T, Price TL, McKeel DW, Morris JC, Growdon JH, Hyman BT. Profound loss of layer II entorhinal cortex neurons occurs in very mild Alzheimer's disease. *J Neurosci*. 1997;16:4491–4500.
- Ohnishi T, Hoshi H, Nagamachi S, et al. High-resolution SPECT to assess hippocampal perfusion in neuropsychiatric diseases. *J Nucl Med*. 1995;36:1163–1169.
- Julin P, Lindqvist J, Svensson L, Slomka P, Wahlund LO. MRI-guided SPECT measurements of medial temporal lobe blood flow in Alzheimer's disease. *J Nucl Med*. 1997;38:914–919.
- Rodriguez G, Nobili F, Copello F, et al. ^{99m}Tc-HMPAO regional cerebral blood flow and quantitative electroencephalography in Alzheimer's disease: a correlative study. *J Nucl Med*. 1999;40:522–529.
- Rombouts SA, Barkhof F, Witter MP, Scheltens P. Unbiased whole-brain analysis of gray matter loss in Alzheimer's disease. *Neurosci Lett*. 2000;19:285:231–233.
- Kitayama N, Matsuda H, Ohnishi T, et al. Measurements of both hippocampal blood flow and hippocampal gray matter volume in the same individuals with Alzheimer's disease. *Nucl Med Commun*. 2001;22:473–477.
- Ishii K, Sasaki M, Yamaji S, Sakamoto S, Kitagaki H, Mori E. Paradoxical hippocampus perfusion in mild-to-moderate Alzheimer's disease. *J Nucl Med*. 1998;39:293–298.
- Ibanez V, Pietrini P, Alexander GE, et al. Regional glucose metabolic abnormalities are not the result of atrophy in Alzheimer's disease. *Neurology*. 1998;50:1585–1593.
- Geddes JW, Monaghan DT, Cotman CW, Lott IT, Kim RC, Chui HC. Plasticity of hippocampal circuitry in Alzheimer's disease. *Science*. 1985;230:1179–1181.
- Hyman BT, Kromer LJ, Van Hoesen GW. Reinnervation of the hippocampal perforant pathway zone in Alzheimer's disease. *Ann Neurol*. 1987;21:259–267.
- Ishii K, Sasaki M, Yamaji S, Sakamoto S, Kitagaki H, Mori E. Demonstration of decreased posterior cingulate perfusion in mild Alzheimer's disease by means of H₂¹⁵O positron emission tomography. *Eur J Nucl Med*. 1997;24:670–673.
- Small GW, Ercoli LM, Silverman DH, et al. Cerebral metabolic and cognitive decline in persons at genetic risk for Alzheimer's disease. *Proc Natl Acad Sci USA*. 2000;97:6037–6042.
- Mazziotta JC, Phelps ME. Principles and applications for the brain and heart. In: Phelps ME, Mazziotta JC, Schelbert H, eds. *Positron Emission Tomography and Autoradiography*. New York, NY: Raven Press; 1986:493–579.
- Meguro K, Blaizot X, Kondoh Y, Le Mestric C, Baron JC, Chavoix C. Neocortical and hippocampal glucose hypometabolism following neurotoxic lesions of the entorhinal and perirhinal cortices in the non-human primate as shown by PET: implications for Alzheimer's disease. *Brain*. 1999;122:1519–1531.
- Desgranges B, Baron JC, de la Sayette V, et al. The neural substrates of memory systems impairment in Alzheimer's disease: a PET study of resting brain glucose utilization. *Brain*. 1998;121:611–631.
- Valenstein E, Bowers D, Verfaellie M, Heilman KM, Day A, Watson RT. Retrosplenial amnesia. *Brain*. 1987;110:1631–1646.
- Papez JW. A proposed mechanism of emotion. *Arch Neurol Psychiatry*. 1937;38:725–743.
- Duara R, Grady C, Haxby JV, et al. PET in Alzheimer's disease. *Neurology*. 1986;36:879–887.
- Salmon E, Gregoire MC, Delfiore G, Lemaire C, et al. Combined study of cerebral glucose metabolism and [¹¹C]methionine accumulation in probable Alzheimer's disease using positron emission tomography. *J Cereb Blood Flow Metab*. 1996;16:399–408.
- Van Hoesen GW, Parvizi J, Chu CC. Orbitofrontal cortex pathology in Alzheimer's disease. *Cereb Cortex*. 2000;10:243–251.